A distinct role of STING in regulating glucose homeostasis through insulin sensitivity and insulin secretion

Jingting Qiao[a,1], Ziyin Zhang[b,c,1], Shuhui Ji[a,d,1], Tengli Liu[e,f], Xiaona Zhang[a], Yumeng Huang[a], Wenli Feng[a], Kunling Wang[a], Jianyu Wang[a], Shusen Wang[e,f], Zhuo-Xian Meng[b,c,g,2], and Ming Liu[a,d,2]

[a]Department of Endocrinology and Metabolism, Tianjin Medical University General Hospital, Tianjin 300052, China; [b]Department of Pathology and Pathophysiology, Zhejiang University School of Medicine, Hangzhou 310058, China; [c]Zhejiang Provincial Key Laboratory of Pancreatic Disease of the First Affiliated Hospital, Zhejiang University School of Medicine, Hangzhou 310058, China; [d]Tianjin Research Institute of Endocrinology, Tianjin 300052, China; [e]Organ Transplant Center, Tianjin First Central Hospital, Tianjin 300192, China; [f]National Health Commission Key Laboratory for Critical Care Medicine, Tianjin First Central Hospital, Tianjin 300384, China; and [g]Department of Geriatrics, Affiliated Hangzhou First People's Hospital, Zhejiang University School of Medicine, Hangzhou 310006, China

Edited by Zhijian Chen, Department of Molecular Biology, The University of Texas Southwestern Medical Center, Dallas, TX; received January 29, 2021; accepted December 14, 2021

Insulin resistance and β-cell dysfunction are two main molecular bases yet to be further elucidated for type 2 diabetes (T2D). Accumulating evidence indicates that stimulator of interferon genes (STING) plays an important role in regulating insulin sensitivity. However, its function in β-cells remains unknown. Herein, using global STING knockout (STING$^{-/-}$) and β-cell–specific STING knockout (STING-βKO) mouse models, we revealed a distinct role of STING in the regulation of glucose homeostasis through peripheral tissues and β-cells. Specially, although STING$^{-/-}$ beneficially alleviated insulin resistance and glucose intolerance induced by high-fat diet, it surprisingly impaired islet glucose-stimulated insulin secretion (GSIS). Importantly, STING is decreased in islets of db/db mice and patients with T2D, suggesting a possible role of STING in β-cell dysfunction. Indeed, STING-βKO caused glucose intolerance due to impaired GSIS, indicating that STING is required for normal β-cell function. Islet transcriptome analysis showed that STING deficiency decreased expression of β-cell function–related genes, including Glut2, Kcnj11, and Abcc8, contributing to impaired GSIS. Mechanistically, the assay for transposase-accessible chromatin with high-throughput sequencing (ATAC-seq) and cleavage under targets and tagmentation (CUT&Tag) analyses suggested that Pax6 was the transcription factor that might be associated with defective GSIS in STING-βKO mice. Indeed, Pax6 messenger RNA and protein levels were down-regulated and its nuclear localization was lost in STING-βKO β-cells. Together, these data revealed a function of STING in the regulation of insulin secretion and established pathophysiological significance of fine-tuned STING within β-cells and insulin target tissues for maintaining glucose homeostasis.

STING | β-cells | insulin resistance | insulin secretion | T2D

Glucose homeostasis is maintained mainly by the precise regulation of insulin secretion from β-cells and insulin action in the insulin target tissues. Genetic and environmental factors that impair insulin secretion and/or action can disrupt glucose homeostasis and lead to metabolic diseases, including type 2 diabetes (T2D). Over the past decades, the prevalence of T2D has been dramatically rising largely due to overnutrition- and low physical activity–induced obesity. However, the underlying mechanisms of obesity-induced metabolic diseases remain to be elucidated. In most mammals, metabolic homeostasis and the immune system interact and influence each other in multiple ways (1, 2). Overnutrition can activate the immune response and induce low-grade chronic inflammation, which is now recognized as an important etiological component in the development of insulin resistance and β-cell dysfunction (1, 3, 4).

The DNA-sensing stimulator of interferon genes (STING) mediates type I interferon inflammatory responses in immune cells, leading to the activation of a protective, antiviral cascade signaling (5–12). In addition to pathogen-derived DNA from microbial infection, recent studies have suggested that under certain pathological conditions, STING could also recognize self-DNA exposed in the cytoplasm of cells, including DNA leaked from the nucleus and cytosolic mitochondrial DNA (mtDNA), and caused autoimmune or autoinflammatory diseases (7, 12–16). STING could also regulate inflammation and immune response in multiple diseases through interacting with transcription factors such as IRF3 (interferon regulatory factor 3), and nuclear factor erythroid 2–related factor 2 (7, 17). More recently, accumulating evidence suggests that STING plays an important role in regulating energy homeostasis and metabolic pathways (18, 19). The STING in mouse adipose tissue can activate high-fat diet (HFD)–induced mtDNA release, leading to an increase of chronic inflammation and insulin resistance (20, 21). Besides

Significance

The role of STING in maintaining glucose homeostasis remains unknown. Herein, using global and β-cell–specific STING knockout mouse models, we revealed a distinct role of STING in the regulation of glucose homeostasis through β-cells and peripheral tissues. Specially, while global STING knockout beneficially alleviated insulin resistance and glucose intolerance induced by high-fat diet, it surprisingly impaired islet glucose-stimulated insulin secretion (GSIS). Further analyses revealed that STING deficiency down-regulated expression of β-cell key transcription factor Pax6, impairing Pax6 nuclear localization and binding activity to the promoters of its target genes, including Glut2 and Abcc8, causing impaired GSIS. These data highlight pathophysiological significance of fine-tuned STING signaling in β-cells and insulin target tissues for maintaining glucose homeostasis.

Author contributions: J.Q. and M.L. designed research; J.Q., Z.Z., S.J., and J.W. performed research; T.L. and S.W. contributed new reagents/analytic tools; J.Q., Z.Z., and Z.-X.M. analyzed data; and J.Q., X.Z., Y.H., W.F., K.W., Z.-X.M., and M.L. wrote the paper.

The authors declare no competing interest.

This article is a PNAS Direct Submission.

[1]J.Q., Z.Z., and S.J. contributed equally to this work.

[2]To whom correspondence may be addressed. Email: mingliu@tmu.edu.cn or zxmeng@zju.edu.cn.

This article contains supporting information online at http://www.pnas.org/lookup/suppl/doi:10.1073/pnas.2101848119/-/DCSupplemental.

Published February 10, 2022.

mediating obesity-induced insulin resistance in adipose tissue, activation of the STING pathway has also been implicated in other metabolic diseases, including nonalcoholic fatty liver disease (NAFLD) (22–24). Consistently, our previous study confirmed that the activation of the STING pathway not only promoted hepatocyte inflammation and apoptosis but also induced glucose metabolism disorder in NAFLD (25). These findings reveal that activation of the STING pathway may be involved in obesity-induced inflammation and metabolic dysfunction, beyond its well-characterized roles in innate immune surveillance.

More recently, STING was found to be expressed in the islets and associated with lipotoxicity-induced inflammation and β-cell apoptosis in vitro (26, 27). However, the role of STING in islets under physiological and pathological conditions remains unknown. In this study, using global STING knockout (KO) (STING$^{-/-}$) mice and β-cell–specific STING KO (STING-βKO) mice, we explored the role of STING in the regulation of glucose homeostasis. We found that although whole-body KO of STING attenuated overall glucose intolerance due to alleviation of HFD-induced insulin resistance in the peripheral tissues, STING deficiency surprisingly impaired β-cell glucose-stimulated insulin secretion (GSIS). The role STING in the regulation of GSIS was further confirmed in STING-βKO mice. Down-regulation of β-cell function–related genes, including Glut2 (glucose transport 2), Kcnj11, and Abcc8, as well as defective intracellular calcium signaling, appeared to be responsible for the impairment of GSIS. Mechanistically, using assay for transposase-accessible chromatin with high-throughput sequencing (ATAC-seq) and cleavage under targets and tagmentation (CUT&Tag) analyses, we identified that Pax6, which is an important transcription factor in maintaining β-cell function (28–30), might be associated with β-cell dysfunction caused by STING deficiency. Consistently, STING deficiency not only down-regulated expression of Pax6 messenger RNA (mRNA) and protein but also caused a loss of nuclear localization. Taken together, these results demonstrated that Pax6 down-regulation, loss of nuclear localization, and impairment of transcriptional activity may be associated with the defective GSIS in STING-βKO islets. Importantly, we found that STING is highly expressed in the islets compared with that of pancreatic exocrine, and the expression of STING was markedly decreased in the islets of patients with T2D and db/db mice, suggesting that STING deficiency may underlie defective insulin secretion during the development and the progression of T2D.

Taken together, these data revealed a function of STING in β-cells and established its distinct role in the regulation of glucose homeostasis through insulin secretion from β-cells and insulin action in the peripheral insulin target tissues. Fine-tuned STING signaling in β-cells and the peripheral tissues is critical for maintaining systemic glucose homeostasis.

Results

Global STING KO Alleviated Glucose Intolerance and Insulin Resistance Induced by HFD. To determine the role of STING in the regulation of glucose homeostasis under metabolic stress, we subjected the global STING KO (STING$^{-/-}$) mice (31) and their littermate controls (Fig. 1*A*) to HFD for 12 wk. Although STING$^{-/-}$ did not affect body weight and fasting blood glucose in the mice fed with normal chow or HFD (Fig. 1 *B* and *C*), STING deficiency significantly improved glucose intolerance induced by HFD (Fig. 1 *D* and *E*). Importantly, neither basal insulin nor glucose induced insulin secretion was increased in STING$^{-/-}$ mice. Although no statistically significant difference was achieved, there was a trend toward decreased serum insulin levels, as measured by an intraperitoneal glucose tolerance test (IPGTT) (Fig. 1*F*). Moreover, no significant differences in serum glucagon levels were observed between STING$^{-/-}$ mice and control mice fed with HFD (Fig. 1*G*). These data suggest that the improvement in IPGTT results in STING$^{-/-}$ mice was not due to improved islet function. Indeed, an intraperitoneal insulin tolerance test (IPITT) showed that STING$^{-/-}$ mice were more sensitive to insulin than control mice fed with HFD (Fig. 1 *H* and *I*). In addition, consistent with previous reports, serum triglyceride and cholesterol levels were lower in HFD-fed STING$^{-/-}$ mice than in control mice (*SI Appendix*, Fig. S1 *A–D*). Meanwhile, although HFD caused impaired phosphorylation of AKT (a key kinase in insulin signaling pathways) in the liver and epididymal white adipose tissue (eWAT) of control mice, STING deletion resulted in increased AKT phosphorylation in liver and eWAT (Fig. 2 *A–F*), suggesting that STING deletion in peripheral insulin target tissues results in metabolic improvement by alleviating insulin resistance induced by HFD. Together, these results established that STING KO improves insulin sensitivity, thereby attenuating HFD-induced glucose intolerance.

Global STING KO Causes an Impairment of GSIS. Insulin secretion in vivo can be affected by both β-cell function and the requirement of insulin to control blood glucose levels. Because we found that STING$^{-/-}$ could improve insulin sensitivity (Figs. 1 *H* and *I* and 2 *A–F*), we reasoned that a trend of low levels of serum insulin (Fig. 1*F*) in STING$^{-/-}$ mice fed with HFD compared with that of control mice may be due to the decreased requirement of insulin. To determine the role of STING in insulin secretion and minimize the possible effect of insulin sensitivity of peripheral tissues on insulin secretion, we isolated islets from STING$^{-/-}$ and control mice and stimulated islets with high glucose. To our surprise, STING deficiency actually resulted in an impairment of GSIS (Fig. 2*G*), without a decrease in islet insulin content (*SI Appendix*, Fig. S2 *A–C*). To further dissect the causes of defective insulin secretion, we stimulated islets with a high concentration of potassium chloride (KCl) and found that STING deficiency also led to impaired KCl-stimulated insulin secretion (KSIS) (Fig. 2*H*). These data suggest that global deletion of STING does not decrease intraislet insulin content but impairs insulin secretion in response to high glucose and KCl.

STING Is Down-Regulated in Pancreatic Islets of db/db Mice and T2D Patients. Progressive β-cell dysfunction featured by impairment of GSIS is a hallmark of T2D. Because STING deficiency results in an impaired GSIS (Fig. 2*G*), it is important to know whether there is a STING deficiency in islets of T2D and whether this deficiency is associated with defective β-cell function in T2D. We therefore firstexamined the expression of STING and its upstream and downstream pathways, including cGAS (cyclic guanosine/adenosine monophosphate synthase), TBK1 (TANK-binding kinase 1), IRF3 (interferon regulatory factor 3), ISG15 (interferon-stimulated gene 15), and interferon-β in the islets of db/db mice. As expected, the db/db mice developed diabetes and hyperlipidemia at age of 8 wk (*SI Appendix*, Fig. S3). We found that mRNA expression of STING and its associated pathways were all significantly down-regulated in islets of db/db mice compared to controls (Fig. 3 *A–C*). The protein levels of STING and TBK1 were also decreased, although no significant changes were found for the ratio of phosphorylated TBK1 to total TBK1 (*SI Appendix*, Fig. S7 *A–C*), suggesting that deficiency of STING-TBK1 signaling in db/db mice may be mainly due to the down-regulation in gene transcription. Immunofluorescence staining and confocal analysis showed that STING was highly expressed in pancreatic islets, mostly in β-cells and α-cells. No detectable STING signal was found in δ-cells. STING was found to be markedly decreased in the β-cells of db/db mice, while no significant change in STING expression was observed in other islet

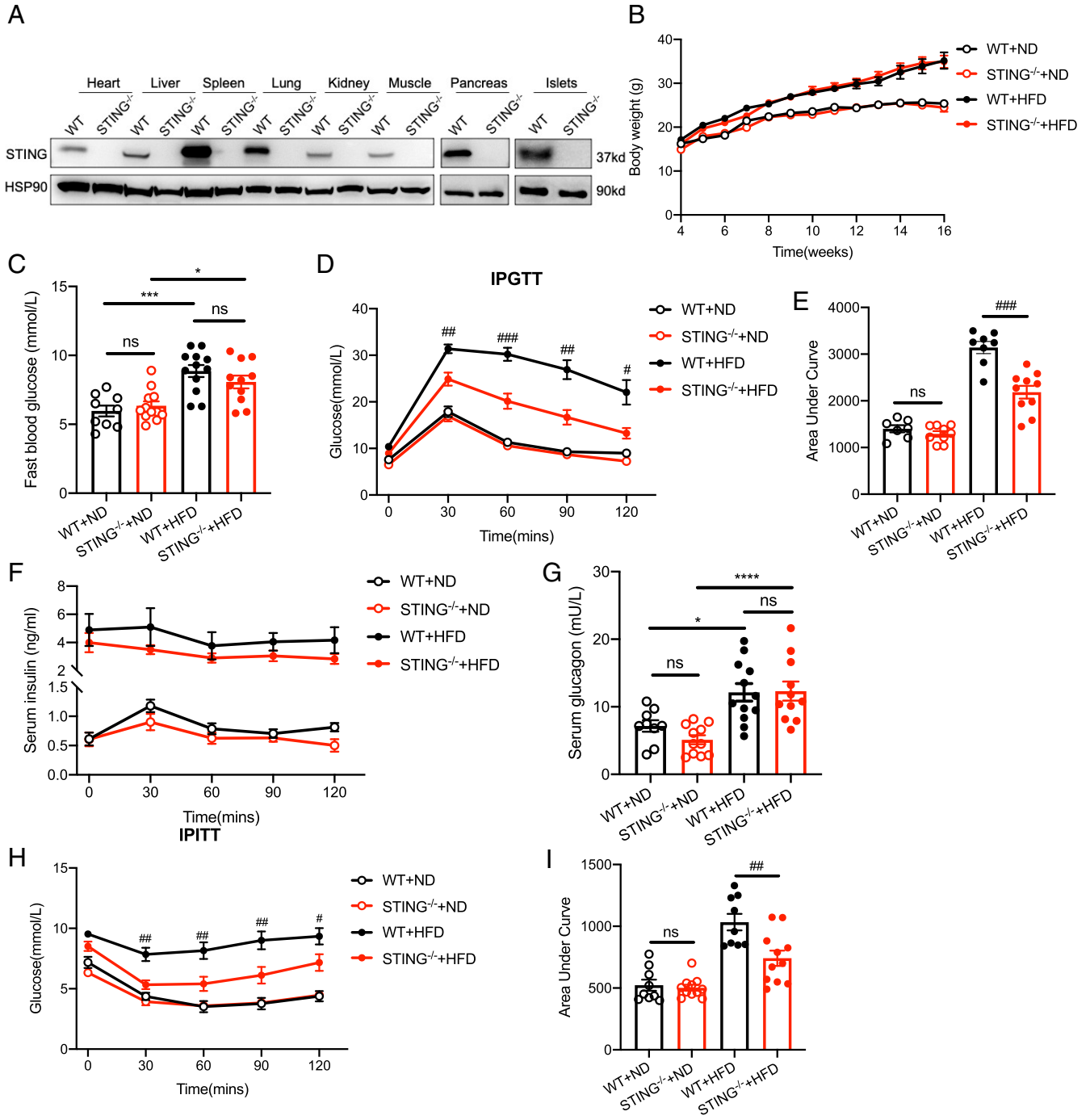

Fig. 1. Global STING KO attenuated HFD-induced insulin resistance and glucose intolerance. (*A*) Verifying the efficiency of STING KO in multiple tissues (heart, liver, spleen, lung, kidney, muscle, pancreas, and islets). (*B*) Four groups of male mice at 4 wk of age were fed HFD or ND for 12 wk. Body weight was monitored once per week (n = 5–12 mice/group). (*C*) Fasting blood glucose after HFD (n = 9–12 mice/group). (*D*) IPGTT performed after 12 wk of HFD (2 g/kg intraperitoneally, n = 7–10 mice/group). (*E*) The total insulin secretion area under the curve (AUC) was calculated from *D*. (*F*) Serum insulin levels in four groups of male mice during the IPGTT were measured by ELISA (n = 4–5 mice/group). (*G*) Fasting serum glucagon levels in four groups of male mice were measured by ELISA (n = 9–12 mice/group). (*H*) IPITT was performed after HFD or ND for 12 wk (0.75 U/kg intraperitoneally, n = 9–11 mice/group). (*I*) The AUC was calculated from *H*. Values are shown as mean ± SEM. WT + ND vs. WT + HFD, STING$^{-/-}$ + ND vs. STING$^{-/-}$ + HFD: $^{*}P < 0.05$, $^{***}P < 0.001$, $^{****}P < 0.0001$; WT + HFD vs. STING$^{-/-}$ + HFD: $^{\#}P < 0.05$, $^{\#\#}P < 0.01$, $^{\#\#\#}P < 0.001$, ns, not significant.

cells, including α- and δ-cells (Fig. 3 *B–D*). To further explore the changes of STING during the development and the progression of diabetes, we isolated islets from different diabetic stages of db/db mice and examined the expression of STING and its correlation with proinsulin folding and insulin content. Consistent with our previous reports (32, 33), as blood glucose levels progressively rose, there was a dramatic increase in misfolded proinsulin levels in db/db mice (Fig. 4*A*, *Upper*). Importantly, gradually increased misfolded proinsulin levels appeared to be linked to an increased ratio of proinsulin to insulin, along with decreased insulin content,

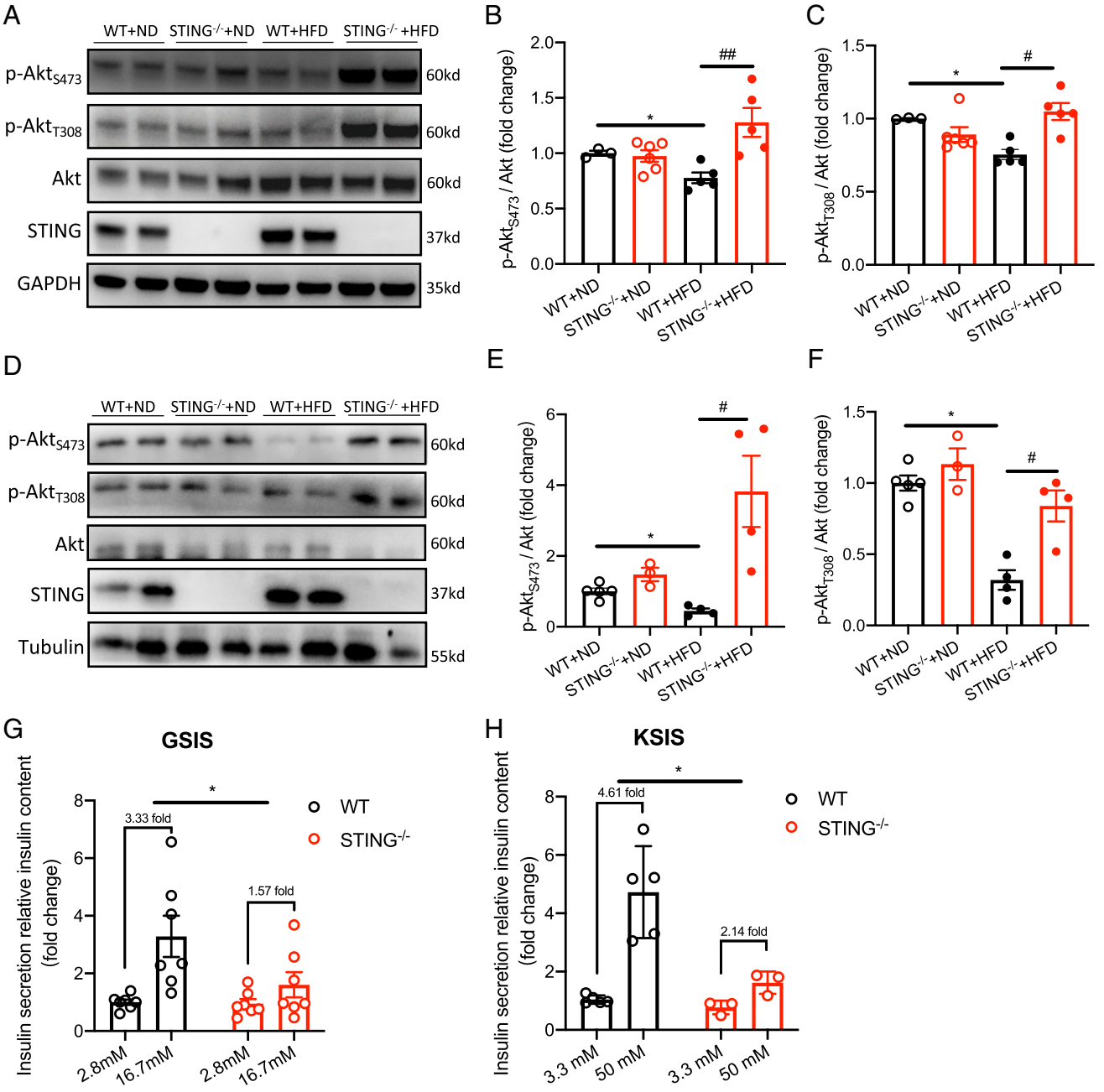

Fig. 2. Global STING KO improved Akt phosphorylation in liver and eWAT of HFD-fed mice but impaired glucose/potassium-stimulated insulin secretion. (*A*) Liver from 16-wk-old male mice were directly lysed. Western blots were performed to examine STING and total Akt, as well as phosphorylated Akt, including $pAkt_{S473}$ and $pAkt_{T308}$. (*B* and *C*) The ratios of $pAkt_{S473}$ or $pAkt_{T308}$ and total Akt were calculated from Fig. 2*A*, and the ratios of islets from control mice fed with ND were set as 1. (*D*) eWAT from 16-wk-old male mice was directly lysed. Western blots were performed to detect $pAkt_{S473}$, $pAkt_{T308}$, Akt, and STING. (*E* and *F*) The ratios of $pAkt_{S473}$ or $pAkt_{T308}$ and total Akt were calculated from Fig. 2*D*, and the ratios of eWAT from control mice fed with ND were set as 1. (*G* and *H*). Isolated islets from 8-wk-old male WT and $STING^{-/-}$ mice were incubated overnight. GSIS or KSIS were performed as described in Materials and Methods. Secreted insulin normalized by islet insulin content was measured by ELISA. n ≥ 3 mice/group. Values are shown as mean ± SEM. WT vs. $STING^{-/-}$, WT + ND vs. WT + HFD: $^{*}P < 0.05$; WT + HFD vs. $STING^{-/-}$ + HFD: $^{\#}P < 0.05$, $^{\#\#}P < 0.01$.

over time (Fig. 4*A*, *Middle*, and Fig. 4*B*). Remarkably, decreased STING occurred even at the prediabetic stage in db/db mice, and a progressive loss of STING was evident as diabetes progressed (Fig. 4 *A* and *C*). Further, in islets of patients with T2D, the expression of STING was also lower than that of nondiabetic controls (Fig. 4*D*). Altogether, given the critical role of STING in GSIS (Fig. 2*G*), the data from db/db mice and patients with T2D suggest that progressive STING deficiency in islets may play an important role in defective insulin secretion in T2D.

β-Cell–Specific STING KO Causes Glucose Intolerance Linked to Decreased Blood Insulin during IPGTT. To further elucidate the distinct physiological role of STING in β-cells, we generated a β-cell–specific STING KO mouse model using the method of homologous recombination mediated genome editing with Cre recombinase driven by rat *Ins2* promoter (RIP-Cre) (34) (*SI Appendix*, Fig. S4). As shown in Fig. 5 *A* and *B*, specific down-regulation of STING expression was achieved only in the islets of $STING^{fl/fl}$; RIP-Cre (STING-βKO) mice, but not in other

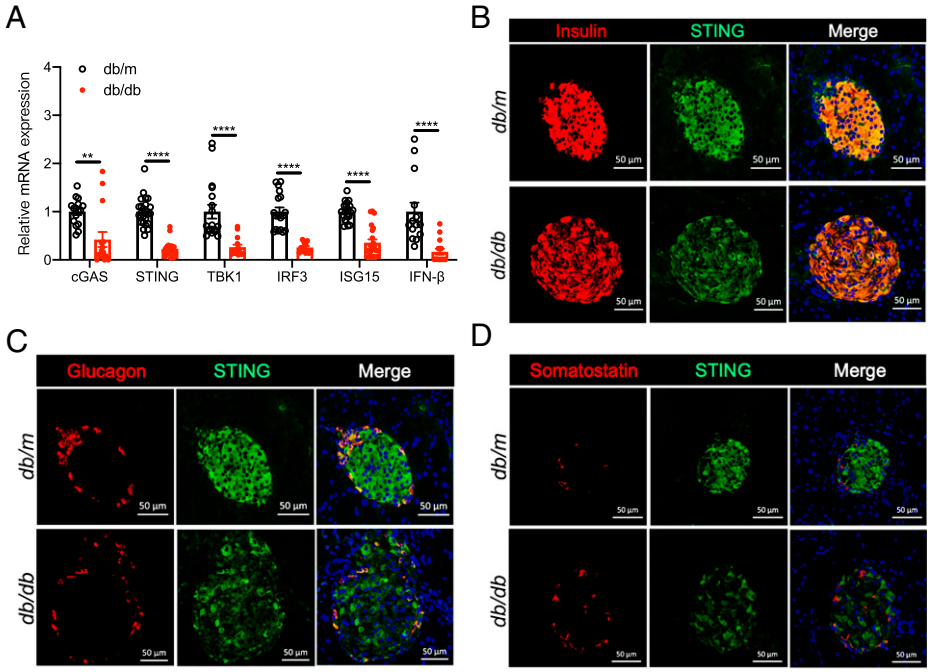

Fig. 3. STING is highly expressed in the islets and the expression of STING, and its upstream/downstream genes were downregulated in db/db islets. (*A*) Isolated islets from 8-wk-old db/db mice and littermate controls were used to analyze the expression of the genes in STING pathway, including cGAS, STING, TBK1, IRF3, ISG15, and interferon-β (IFN-β), using Real-Time Quantitative PCR (RT-QPCR). n ≥ 3 mice/group. The STING expression in β-cells (*B*), α-cells (*C*), and δ-cells (*D*) in islets from 6- to 8-wk-old db/db mice and littermate controls was detected via the immunofluorescent staining with anti-insulin (red), anti-glucagon (red), anti-somatostatin (red), anti-STING (green) antibodies, and DAPI (blue). n = 3 mice/group. Values are shown as mean ± SEM. $^{**}P < 0.01$; $^{****}P < 0.0001$. (Scale bars, 50 μm.)

tissues examined, including hypothalamus (*SI Appendix*, Fig. S5). STING-βKO did not affect mouse body weight and fasting blood glucose (Fig. 5 *C* and *D*). However, when the male mice were challenged with high glucose during the IPGTT, STING-βKO led to glucose intolerance demonstrated by markedly increased blood glucose during the IPGTT (Fig. 5 *E* and *F*). This impairment of glucose tolerance appeared to be directly linked to decreases of blood insulin when the mice were challenged with glucose (Fig. 5*G*). The insulin sensitivity did not change in STING-βKO male mice (Fig. 5*H*). Similar results were also confirmed in the STING-βKO female mice (*SI Appendix*, Fig. S6 *A–F*). These data strongly support the notion that STING plays an important role in β-cell function and STING deficiency can lead to impaired glucose intolerance due to insufficient blood insulin level in response to glucose challenge.

β-Cell–Specific STING KO Does Not Affect Insulin Expression but Impairs GSIS. To determine whether the decreased insulin in blood (Fig. 5*G*) is caused by decreased insulin biosynthesis/storage or a defect in insulin secretion, we isolated islets from STING-βKO mice and examined expression of insulin mRNA and insulin content. No changes in insulin expression (Fig. 6*A*), insulin content (Fig. 6 *B–E*), or secretory granules (Fig. 6*F*) were found in the islets of STING-βKO mice, indicating that STING does not affect insulin biosynthesis and storage. However, consistent with the results in the global STING KO mice, STING-βKO also led to impaired GSIS (Fig. 6*G*). To examine whether STING-TBK1 signaling directly regulates GSIS, we treated isolated islets with STING or TBK1 inhibitors and found that inhibiting STING-TBK1 signaling indeed impaired GSIS (*SI Appendix*, Fig. S7*D*). However, inhibition of nuclear factor κB did not appear to affect insulin secretion in β-cells (*SI Appendix*, Fig. S7*E*). Normal GSIS requires multiple signaling pathways involved in glucose transport, glucose metabolism, potassium channel closing, and calcium influx. To dissect the defects of GSIS, we performed islet perfusion to examine dynamics of insulin secretion in response to both high glucose and KCl. We found that STING-βKO islets not only had impaired insulin secretion in response to high glucose but also exhibited defective insulin secretion induced by membrane depolarization with a high K^+ concentration (Fig. 6 *H–J*). In addition, fluorescence-based whole-islet Ca^{2+} imaging showed that the intracellular Ca^{2+} response to glucose stimulation was significantly decreased (Fig. 6*K*). Collectively, these results suggest that STING plays an important role in maintaining normal β-cell function mainly through the regulation of insulin secretion rather than insulin biosynthesis and storage.

β-Cell–Specific STING Deficiency Decreases the Expression of β-Cell Function–Related Genes. To further determine the pathways that may contribute to the impairment of GSIS and KSIS, we performed transcriptome analysis using isolated islets from STING-βKO mice and found 1,615 significantly changed genes [average fragments per kilobase of transcript per million mapped reads (FPKM) > 1; $|\log_2 FC| > 1$; $q < 0.05$) in islets between STING-βKO mice and littermate controls (Fig. 7*A*). Gene Ontology (GO) analysis of the transcriptome showed that 31 genes associated with insulin secretion, 34 genes associated with potassium ion transport, and 59 genes associated with the regulation of protein secretion were significantly altered in the islets of STING-βKO mice compared with control mice (Fig. 7*B*). We further used RT-QPCR to examine the expression of some key transcription factors, enzymes, glucose transports, and ion channels that are critical for insulin biosynthesis and secretion. We found that mRNA expression of Pdx1 and MafA [two key transcription factors for β-cell function and insulin expression (35, 36)], Nkx6.1 and NeuroD1 [markers of β-cell maturation and function (35)], as well as glucose kinase (the first key kinase for glucose metabolism in β-cells), was not affected by STING deficiency (Fig. 7*C*). However, mRNA expression of Pax6, an essential transcription factor for β-cell function and GSIS (28–30), was decreased in islets of STING-βKO mice (Fig. 7*C*). Meanwhile, the mRNA expression of some important genes involved in positive regulation of GSIS, including Glut2 (encoded by Slc2a2), potassium ion channels (Kcnj11 and Abcc8), potassium calcium-activated channels (Kcnn2 and Kcnn4) (37), adenylate cyclase activating polypeptide 1 (Adcyap1) (38), transient receptor potential cation channel subfamily M member 4 (39), and ATPase Na^+/K^+ transporting subunit alpha 3 were markedly decreased in the islets of

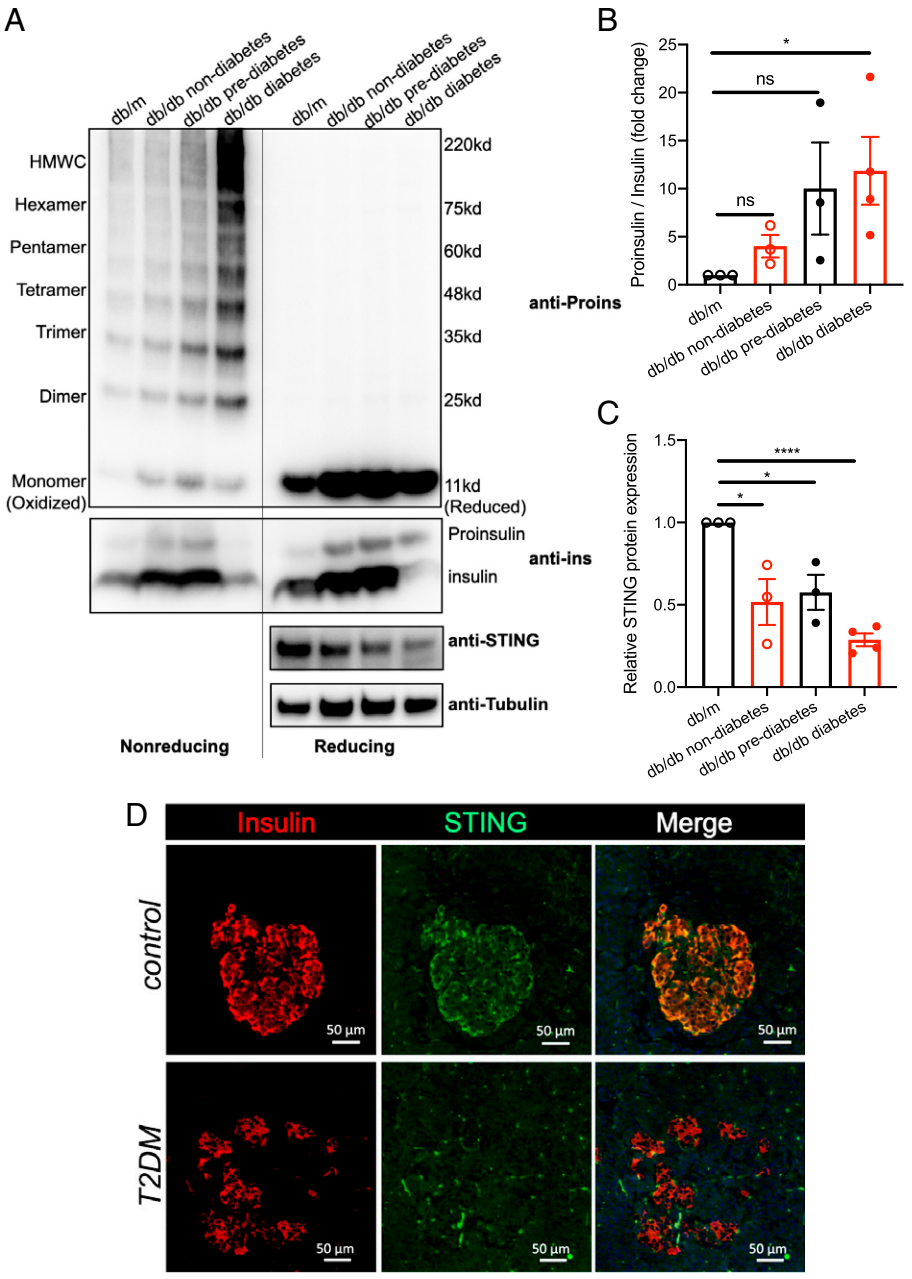

Fig. 4. A progressive loss of STING in the islets of db/db mice during the development/progression of diabetes and decreased STING expression in islets of patients with T2D. (*A*) Freshly isolated islets from db/db mice and littermate controls at age 4–8 wk were directly lysed. The total proteins were resolved in 4–12% gradient gel under nonreducing and reducing conditions and electrotransferred to nitrocellulose membrane, followed by Western blotting with anti-proinsulin (*Upper*), anti-insulin (*Middle*), and anti-STING (*Lower*) as indicated. Tubulin was used as an internal reference. (*B*) Total proinsulin and insulin under reducing conditions from *A* were quantified. The ratios of proinsulin and insulin were calculated, and the ratios of proinsulin/insulin of db/m islets were set as 1. (*C*) STING and tubulin from at least three independent experiments shown in *A* were quantified. The ratios of STING and tubulin were calculated, and the ratio of STING and tubulin of db/m islets was set as 1. n ≥ 3 mice/group. (*D*) Immunofluorescent staining of pancreas sections of donors with or without T2D were performed for anti-insulin (red), anti-STING (green), and DAPI (blue). n = 5 patients per group. Values are shown as mean ± SEM. $*P < 0.05$, $****P < 0.0001$, ns, not significant. (Scale bars, 50 μm.)

STING-βKO mice, whereas the gene negatively associated with insulin secretion, prostaglandin E receptor 3 (40), was increased in the islets of STING-βKO mice (Fig. 7*C*). These data suggest that STING regulates insulin secretion, likely through transcriptional regulation of glucose transporters, ion channels, and genes that are important for normal GSIS.

Identification of Pax6 as the Key Transcriptional Factor Associated with Defective GSIS in STING-βKO Mice. To find the common transcription factor that is shared among STING-regulated genes that are correlated with defective GSIS in STING-βKO islets, we performed the ATAC-seq analysis using isolated islets from STING-βKO and control mice. We identified 3,641 chromatin regions exhibiting accessibility changes by STING inactivation (differential peaks; $|\log_2 FC| > 0.5$, $P < 0.05$, normalized read counts > 0), (Fig. 8*A*), suggesting that STING might affect chromatin remodeling. These differential peaks were further annotated to the 2,888 closest genes that could be potentially regulated by STING in β-cells. Further GO biological process analysis of these 2,888 genes demonstrated significant enrichment of biological pathways, including insulin secretion, glucose homeostasis, and regulation of ion transmembrane transport (*SI Appendix*, Fig. S9*A*). To explore the possible transcription factors that are associated with the chromatin remodeling in islet β-cells from STING-βKO mice, we then performed known motif enrichment analysis on STING-dependent differential peaks and found that binding sites for several β-cell function–related transcription factors such as Foxa2, Isl1, Pdx1, NeuroD1, Nkx6.1, and Pax6 were significantly enriched in these regions (Fig. 8*B*). To test which transcription factor is mainly involved in the regulation of β-cell function–related genes by STING inactivation, we integrated our ATAC-seq datasets and Chip-Seq or CUT&Tag datasets of the above-mentioned transcription factors into the Integrative Genomics Viewer (IGV)

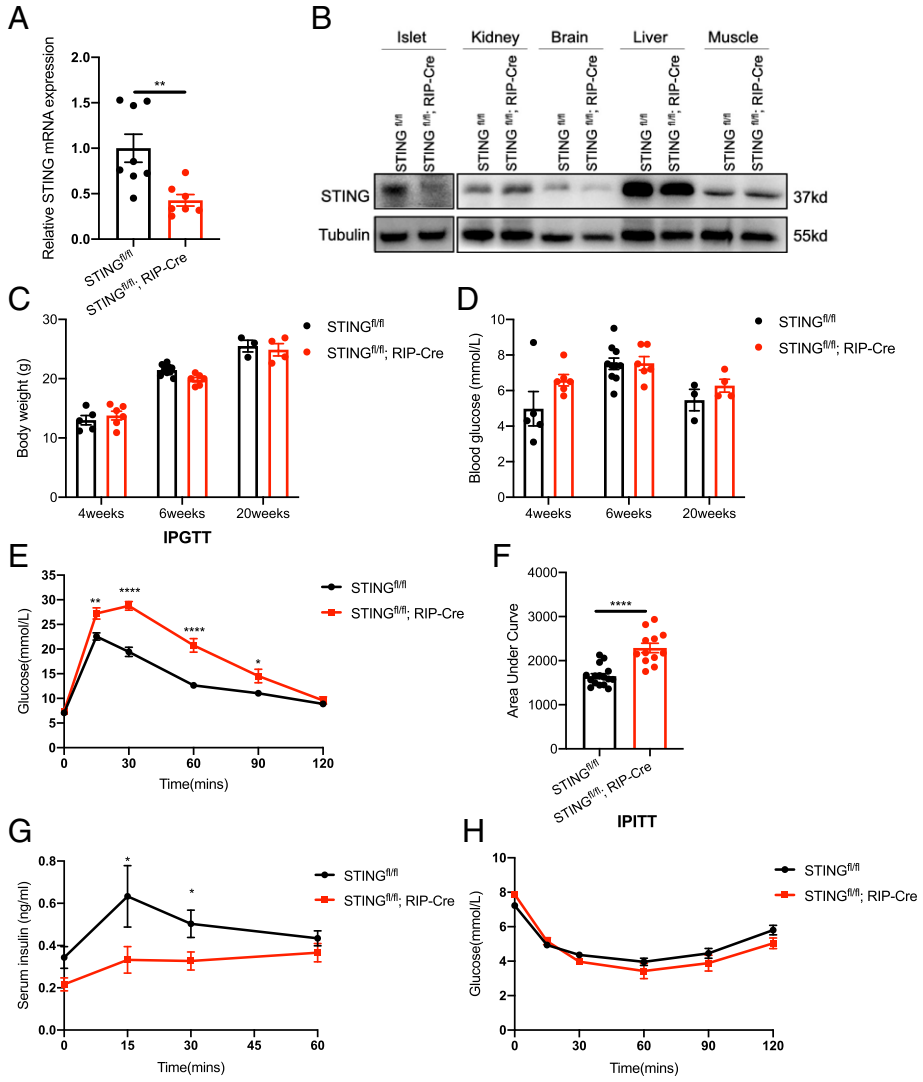

Fig. 5. β-cell–specific STING KO (STING$^{fl/fl}$; RIP-Cre) mice exhibited glucose intolerance and impaired insulin secretion. (*A*) STING mRNA levels in islets of 6-wk-old STING$^{fl/fl}$; RIP-Cre mice and littermate controls were measured by RT-QPCR. (*B*) Freshly isolated islets and indicated tissues from 6-wk-old STING$^{fl/fl}$; RIP-Cre mice and littermate controls were directly lysed. The levels of STING protein were examined in islets, kidney, brain, liver, and muscle. (*C*) Body weight of STING$^{fl/fl}$; RIP-Cre male mice and littermate controls was measured at 4, 6, and 20 wk of age. (*D*) Blood glucose levels of STING$^{fl/fl}$; RIP-Cre male mice and littermate controls were measured at 4, 6, and 20 wk of age. (*E*) An IPGTT was performed in male STING$^{fl/fl}$; RIP-Cre mice and littermate controls at 6 wk of age. (*F*) The AUC of blood glucose during the IPGTT was calculated from *E*. (*G*) Serum insulin in response to intraperitoneal glucose injection during the IPGTT were measured by ELISA. (*H*) An IPITT was performed in 7-wk-old STING$^{fl/fl}$; RIP-Cre male mice and littermate controls. n ≥ 3 mice/group. Values are shown as mean ± SEM. $*P < 0.05$, $**P < 0.01$, $****P < 0.0001$.

to examine their binding profiles on the genes regulated by STING-βKO. We found that the genome browser tracks of ATAC-seq signals on the coding regions and flanking loci of genes critical for β-cell function such as Slc2a2 and Abcc8 were markedly decreased, especially on the enhancer and promoter regions, and that these regions were mainly bound by Pax6 and Nkx6.1 rather than other transcription factors, including Foxa2, Isl1, NeuroD1, and Pdx1 (Fig. 8*C*).

We next examined whether Pax6 expression was also regulated by STING deficiency and found that both mRNA and protein levels of Pax6 were down-regulated in STING-βKO islets (Figs. 7*C* and 8*D*). Consistently, immunofluorescent staining of pancreas sections showed a significant decrease of Pax6 protein levels in STING-βKO islets, while no significant differences were observed in other transcription factors (Pdx1, Isl1, and Nkx6.1) between the two groups (Fig. 8*E* and *SI Appendix*, Fig. S8 *A–C*). More importantly, we observed a loss of nuclear localization of Pax6 protein in STING-βKO islets (Fig. 8*E*), suggesting an important role of STING in the regulation of Pax6 expression and transcriptional activity. To examine whether STING directly or indirectly affects Pax6, we knocked down STING with small interfering RNA (siRNA) or inhibited STING with its inhibitor in β-cells. We found that STING inhibition significantly decreased the expression of Pax6 (*SI Appendix*, Fig. S8 *D* and *E*), suggesting that STING regulates the Pax6 expression in β-cells in a cell-autonomous manner.

Since the mRNA and protein expression of Pax6 was remarkably down-regulated in islets from STING-βKO mice, we next tested whether the genome-wide DNA-binding activity of Pax6 was also altered in islet β-cells by STING ablation using CUT&Tag analysis. As expected, the overall Pax6 DNA-binding activity was impaired in islets from the STING-βKO mice compared to controls (*SI Appendix*, Fig. S9*B*). Among the total 28,467 shared peaks between the two groups, we obtained 695 peaks that were significantly altered ($|\log_2 FC| > 0.5$, $P < 0.05$, normalized read counts > 0; *SI Appendix*, Fig. S9*C*). Interestingly, GO pathway analysis revealed that biological processes such as regulation of carbohydrate metabolic process, positive regulation of insulin secretion, positive regulation of hormone secretion, and positive regulation of sodium ion transport were enriched in genes containing the Pax6-bound peaks that are down-regulated by STING-βKO (*SI Appendix*, Fig. S9*D*), consistent with the above findings in transcriptomic and DNA accessibility levels as revealed by RNA-sequencing (RNA-seq) and ATAC-seq, respectively. More importantly, the genome browser track analysis of Pax6 CUT&Tag data on gene coding regions and flanking loci demonstrated markedly reduced

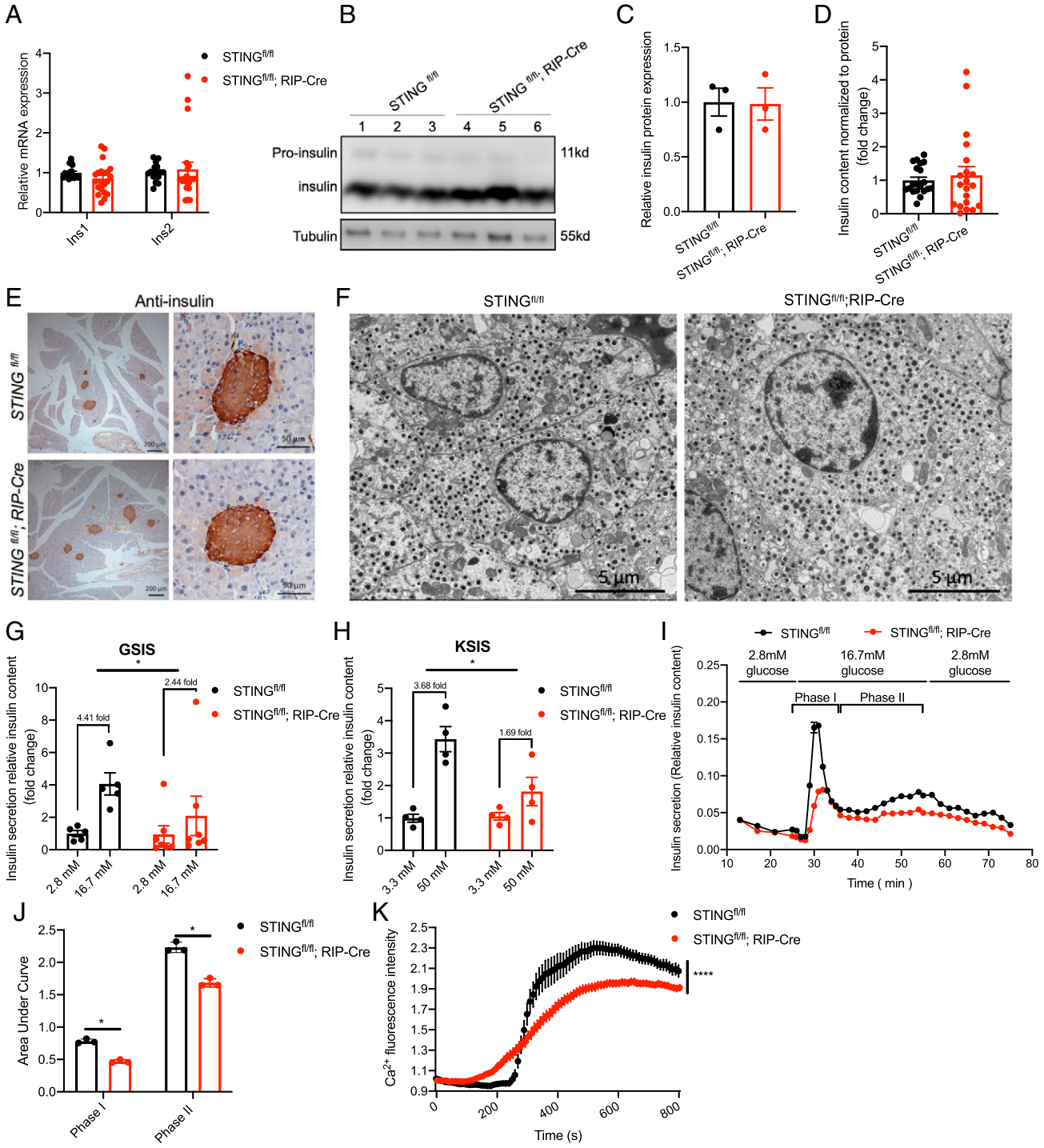

Fig. 6. β-cell–specific STING KO does not affect insulin biosynthesis and storage but impairs GSIS and KSIS. (*A*) mRNA levels of *Ins1* and *Ins2* from islets of STING$^{fl/fl}$; RIP-Cre male mice and littermate controls. (*B* and *C*) Freshly isolated islets from 6-wk-old STING$^{fl/fl}$; RIP-Cre male mice and littermate controls were directly lysed. STING protein levels were examined by Western blotting. Tubulin was used as an internal reference for normalization of STING. (*D*) Insulin content of islets was measured by ELISA. (*E*) STING expression in islets was detected by immunohistochemical staining with anti-insulin. (Scale bars, 200 and 50 μm.) (*F*) Representative electron microscopic images of β-cells from STING$^{fl/fl}$; RIP-Cre mice and littermate controls. (Scale bars, 5 μm.) (*G* and *H*) GSIS and KSIS were performed as described in Materials and Methods. Secreted insulin normalized by islet insulin content was measured by ELISA. (*I*) Dynamic insulin secretion of the STING$^{fl/fl}$; RIP-Cre and STING$^{fl/fl}$ mouse islets cultured in the perfusion chamber with continues buffer renewal. (*J*) Total phase I and phase II insulin secretion was determined by calculating the AUC of islet perifusion. (*K*) Representative image of intracellular Ca^{2+} influx in isolated islets. Ca^{2+} fluorescence intensities were measured in each group of islets when the islets were stimulated with 16.7 mmol/L glucose. n ≥ 3 mice/group. Values are shown as mean ± SEM. *$P < 0.05$, ****$P < 0.0001$.

binding signals on the promoter regions of Slc2a2 and Abcc8 genes in islets from STING-βKO mice compared to control mice (*SI Appendix*, Fig. S8*F*).

Taken together, these results demonstrate that Pax6 is the key transcription factor that may be associated defective GSIS in STING-βKO mice. STING inactivation in β-cells down-regulates

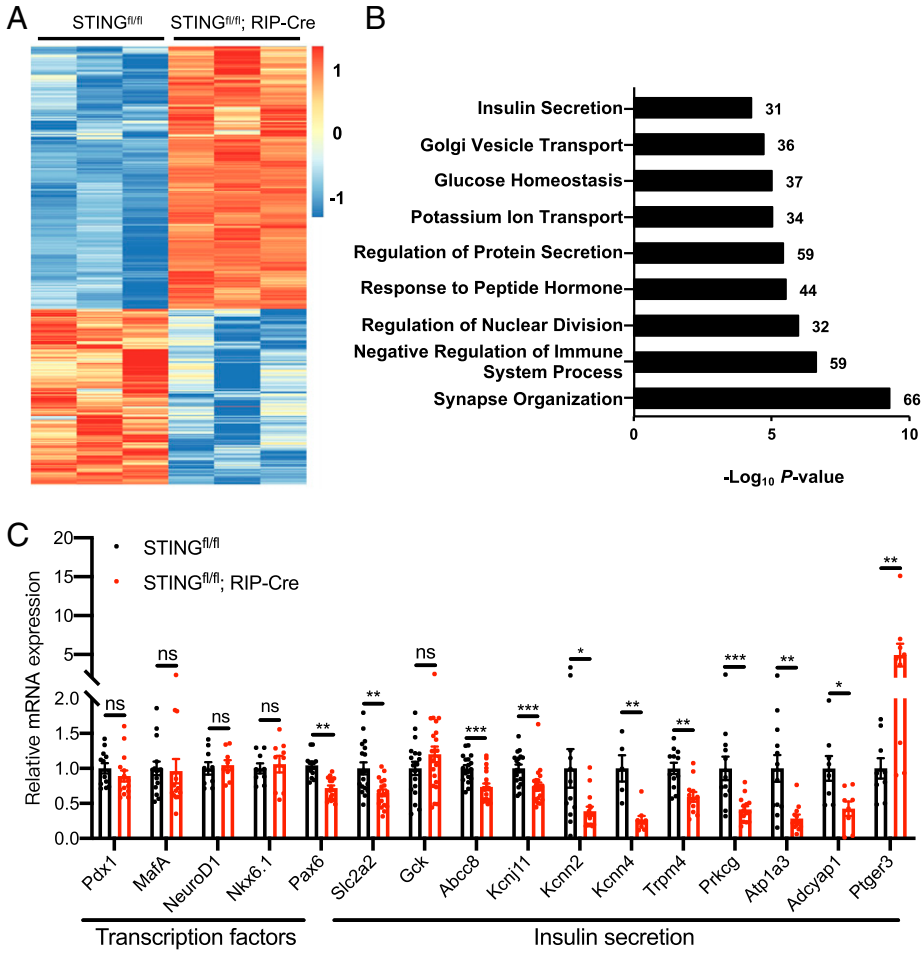

Fig. 7. β-cell–specific STING KO down-regulates expression of genes critical for insulin secretion. (*A*) Heatmap showed scaled, $\log_2$-FPKM (*Z* score) of 1,615 significantly different genes (average FPKM > 1; $|\log_2 FC| > 1$; *P* adjusted < 0.05) in islets between 8-wk-old STING$^{fl/fl}$; RIP-Cre mice and littermate controls. n = 3 mice/group. (*B*) GO analysis of 1,615 significantly different genes in *A*. Most significant and non-redundant biological processes with respective gene numbers and *P* values are shown. (*C*) RT-QPCR analysis of genes related with transcription and insulin secretion in islets from STING$^{fl/fl}$; RIP-Cre mice and littermate controls. n ≥ 3 mice/group. Values are shown as mean ± SEM. **P* < 0.05, ***P* < 0.01, ****P* < 0.001, ns, not significant.

the mRNA and protein expression of Pax6 and decreases the binding activity of Pax6 on the promoter and enhancer regions of genes critical for β-cell function, such as Slc2a2 and Abcc8, thereby leading to impairment of β-cell insulin secretion and systemic glucose homeostasis. However, how STING regulates Pax6 expression and its transcriptional activity in β-cells remains to be explored in a future study.

Discussion

In this study, we explored the role of STING in the regulation of glucose homeostasis under physiological and pathological conditions. Our results demonstrated that STING plays a critical role in not only insulin action in peripheral tissues but also insulin secretion in pancreatic β-cells. Specifically, we found that although global STING deletion ameliorated HFD-induced insulin resistance in peripheral insulin target tissues and improved glucose tolerance, β-cell–specific STING deletion unexpectedly resulted in defective GSIS and glucose intolerance. Using multiple independent genetic and biological approaches, we revealed that STING deletion in β-cells decreased the expression, nuclear localization, and transcription activity of the key β-cell transcription factor Pax6, leading to the down-regulation of glucose transporter Glut2 and potassium ion channels that are critical for β-cell GSIS. These data identify a function of STING in β-cells and highlight pathophysiological significance of fine-tuned STING signaling in β-cells and the peripheral tissues in maintaining systemic glucose homeostasis.

Accumulating evidence indicates that a crosstalk between metabolic signaling and the immune response plays an important role in maintaining energy homeostasis (1, 2). STING appeared to be a key player mediating these interactions between metabolic and immune systems. However, while the pivotal roles of the STING pathway in immune defense against various microbial pathogens have been extensively studied (6–12), its function in nonimmune cells has only been explored recently. STING has been shown to be critical for glucose and lipid metabolism by regulating glycogen and lipid storage (25), as well as cholesterol biosynthesis (41). Activation of the STING pathway mediates obesity-induced inflammation and metabolic disorders. Consistent with these studies, our current work indicates that global STING deletion attenuates HFD-induced insulin resistance and glucose intolerance (Figs. 1 and 2 *A–F* and *SI Appendix*, Fig. S1) (20–25, 42). However, those findings have focused only on peripheral insulin target tissues, including liver and adipose tissues. The function of STING in β-cells remains unknown. In the study, we revealed that STING is highly expressed in the pancreatic islets, especially in islet β-cells and α-cells (Fig. 3 *B–D*), suggesting a possible role of STING in islet function. Indeed, β-cell–specific STING KO did not affect insulin biosynthesis and storage but caused an impairment of GSIS (Fig. 5). These data highlight a distinct role of STING in maintaining glucose homeostasis through the regulation of insulin secretion in β-cells and insulin sensitivity in peripheral insulin target tissues. Although global STING deletion impaired GSIS of β-cells, it alleviated HFD-induced insulin resistance, which appeared to be sufficient

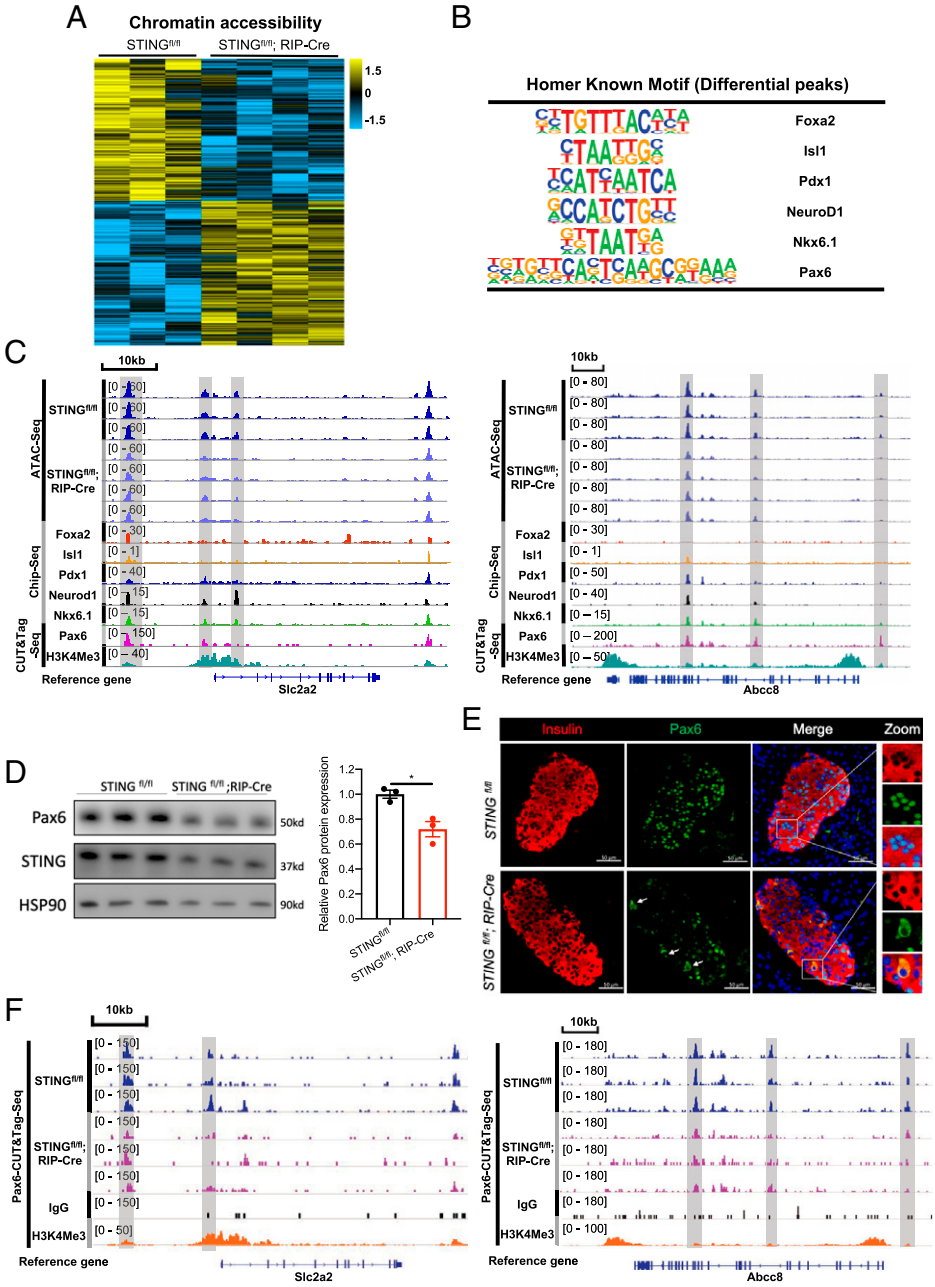

Fig. 8. Pax6 is the key transcriptional factor associated with the defective GSIS in STING-βKO mice. (*A*) Heatmap of chromatin peak accessibility for 3,641 significantly different peaks ($|\log_2 FC| > 0.5$; $P < 0.05$; normalized read counts > 0) in islets between 12-wk-old STING$^{fl/fl}$; RIP-Cre mice and controls. Each row represents a *Z* score of $\log_2$-transferred normalized read counts within each sample using ATAC-seq. (*B*) Known motif search within significantly differential peaks in *A*. Motifs are arranged in rank order according to *P* value. (*C*) Representative ATAC-seq, chromatin immunoprecipitation sequencing, and CUT&Tag-seq genome browser tracks displaying STING-regulated gene loci, including Slc2a2 and Abcc8. (*D*) Expression of Pax6 protein in islets of 8-wk-old STING$^{fl/fl}$; RIP-Cre mice was examined by Western blotting. Relative Pax6 protein level was quantified and calculated (*Right*). (*E*) The expression and intracellular localization of Pax6 in 8-wk-old STING$^{fl/fl}$; RIP-Cre mice and controls were detected by the immunofluorescent staining with anti-insulin (red), anti-Pax6 (green), and DAPI (blue). (Scale bars, 50 μm.) (*F*) Genome browser tracks of Pax6 CUT&Tag-seq signals on two representative STING-regulated gene loci, Slc2a2 and Abcc8. Values are shown as mean ± SEM of at least three independent experiments. $*P < 0.05$.

to offset the impairment of GSIS, resulting an improvement HFD-induced glucose intolerance in global STING KO mice.

A recent study showed that palmitic acid (PA) could increase the expression of STING up to twofold, which could contribute to the PA-induced increase in β-cell death and impairment of GSIS (27). Abolishing PA-induced STING elevation by siRNA-mediated knockdown could decrease cell death and improve insulin secretion defect caused by PA, suggesting that abnormal elevation/activation of STING may impair β-cell survival and function (27). Consistent with that observation, our current study showed that STING KO impaired GSIS, suggesting that a normal level or function of STING plays an important role in insulin secretion in response to high glucose. Together, the previous study and our current work reveal different effects of STING protein under two different conditions: up-regulation/abnormal activation and deletion/inactivation. Both studies highlight the significance of a fine-tuned STING signaling in maintaining the normal function of β-cells.

In β-cells, multiple intracellular steps act in concert to ensure normal GSIS. Upon being transported into β-cells via Glut2, glucose is phosphorylated by the first rate-limiting enzyme (glucokinase) entering glycolytic pathway to produce adenosine triphosphate (ATP), leading to ATP/adenosine diphosphate ratio increases and resulting in closure of ATP-sensitive K^+ channels on the plasma membrane, whereby the membrane depolarizes and voltage-dependent Ca^{2+} channels open, allowing an influx of Ca^{2+} and leading to the exocytosis of insulin (43–45). Defects in any of these steps can impair GSIS. In STING-βKO islets, although there is no change of insulin content (Fig. 6 *A–F*), mRNA expression of Slc2a2 (encoding Glut2) and genes encoding potassium ion channels (Kcnj11, Abcc8, Kcnn2, and Kcnn4) was markedly down-regulated (Fig. 7*C*), suggesting that STING may regulate insulin secretion by modulating the expression of glucose transport and some key ion channel genes, which affects glucose- and potassium-induced membrane depolarization and calcium influx (Fig. 6).

Multiple β-cell key transcription factors (Pdx1, Nkx6.1, Isl1, MafA, and Pax6) have been shown to play important roles in the regulation of genes important for β-cell function. In the effort of searching for a common transcription factor responsible for dysregulation of Slc2a2 and potassium ion channels in STING-βKO mice, Pax6 was identified as a key transcription factor that is correlated with the defective insulin secretion caused by STING inactivation (Figs. 7 and 8 and *SI Appendix*, Figs. S8 and S9). Pax6 is an essential transcription factor for normal islet development and function, especially for GSIS (29, 46). Islet β-cell–specific deletion of Pax6 in adult mice leads to profound diabetes with marked abnormal in insulin secretion, gene expression, glucose metabolism, and Ca^{2+} dynamics (47). Heterozygous mutations of Pax6 are linked to defective insulin secretion, glucose intolerance, and early-onset diabetes in humans (48). However, despite the critical role of Pax6, its regulation in β-cells remains largely unknown. In this study, we found that Pax6 expression, nuclear localization, and binding activities to the promoter regions of its target genes were significantly decreased in STING-βKO mice (Figs. 7 and 8 and *SI Appendix*, Fig. S9). Moreover, directly down-regulation of STING by siRNA (*SI Appendix*, Fig. S8*D*) or inhibition of STING by its inhibitor (*SI Appendix*, Fig. S8*E*) markedly decreased the expression of Pax6 in β-cells. These data suggest that STING may be an important upstream regulator of Pax6, which is associated with the down-regulation of critical genes for insulin secretion, causing defective GSIS in STING deficiency mice.

In summary, this study identifies a pivotal role of STING in insulin secretion from β-cells. Given the fact that STING has a distinct role in β-cells and the peripheral insulin target tissues, it would be important to maintain fine-tuned STING signaling in different tissues. Therefore, for the therapeutic purpose of T2D, targeting the STING pathway may require tissue-specific strategies to achieve beneficial effects in target tissues.

Materials and Methods

Mice. Male wild-type (WT) mice were purchased from SPF Biotechnology. Mice functionally deficient for the long-form leptin receptor (db/db mice) were obtained from Jackson Laboratory. Global STING KO ($STING^{-/-}$) mice were kindly provided by Zhengfan Jiang (School of Life Sciences, Peking University, Beijing, China) (31). For HFD feeding, $STING^{-/-}$ mice and WT mice were randomly divided into four groups and fed either a normal diet [ND; 20% protein; 4% fat; 5% fiber, SCXK (Lu) 2018-0003] or HFD (20% protein; 60% fat, 20% carbohydrate, D12492, Research Diets) for 12 wk. During the period, mice body weight and blood glucose were monitored once a week. STING floxed mice and RIP-Cre mice were purchased from Shanghai Model Organisms Center, Inc., and crossbred to obtain pancreatic β-cell–specific STING KO mice (i.e., $STING^{fl/fl}$; RIP-Cre mice). All mice used were on a C57BL/6J background and housed under a 12-h light/dark cycle in temperature- (22–25 °C) and humidity-controlled (55 ± 5%) rooms.

Islet Isolation and Insulin Secretion Assay. The animals were euthanized and Hanks balanced salt solution containing collagenase P was injected into the common bile duct of the mice. The distended pancreas was isolated and digested for 11 min at 37 °C. Islets were purified by Histopaque-density centrifugation followed by handpick under a dissecting microscope and collected in RPMI medium containing 10% fetal bovine serum, 50 μg/mL streptomycin, and 50 U/mL penicillin. The islets were cultured overnight for further experiments at 37 °C in a humidified 5% CO_2 atmosphere. For GSIS and KSIS assays, the culture medium was removed and the islets were incubated for 1 h in Hepes/balanced Krebs-Ringer bicarbonate buffer (KRBH) (135 mmol/L NaCl, 3.6 mmol/L KCl, 0.5 mmol/L $MgSO_4{\cdot}7\ H_2O$, 0.5 mmol/L NaH_2PO_4, 2 mmol/L $NaHCO_3$, 10 mmol/L Hepes, 1.5 mmol/L $CaCl_2$, and 0.1% BSA) without glucose. Thereafter, the islets were incubated in KRBH containing low glucose (2.8 mmol/L) for 2 h followed by a stimulatory glucose (16.7 mmol/L) for GSIS or KRBH containing low 3.3 mmol/L KCl for 2 h followed by a stimulatory 50 mmol/L KCl at 37 °C for 2 h. Supernatants were collected, and the islets were homogenized in lysis buffer and extracted at 4 °C. The extracts were centrifuged, and islet insulin content and secreted insulin were measured using an enzyme-linked immunosorbent assay (ELISA). The secreted insulin was normalized to insulin content of the islets.

Massive Parallel Sequencing of RNA (RNA-Seq) and Analysis. Islets were sent to BGI Group for RNA extraction, library preparation, and sequencing. In brief, mRNA was enriched from total RNA, fragmentized, and used for reverse transcription and second-strand complementary DNA (cDNA) synthesis. The cDNA was then tailed with adaptors for PCR amplification and sequencing. Data were processed following the standard BGI mRNA analysis pipeline. Statistical analysis was performed with the Deseq2 (v1.28.1) package. Statistical parameters to call differential expressed genes in each analysis are described in Fig. 7 A and B. Unsupervised clustering and heatmap visualization were performed with pheatmap (v1.0.12; https://cran.r-project.org/web/packages/pheatmap/index.html). GO and pathway grouping and enrichment studies were performed by clusterProfiler (V3.16.1) (49), and pathway visualization was conducted using pathview (v1.28.1) (50).

ATAC-seq of Isolated Islets and Analysis. The ATAC-seq protocol was adapted from a previous report (51). In brief, 50,000 cells were extracted from isolated islets by TrypLE (Thermo Fisher, 12604013). Islets were lysed with lysis buffer (10 mM Tris·HCl, pH 7.4, 10 mM NaCl, 3 mM $MgCl_2$, and 0.1% (vol/vol) Igepal CA-630) at 4 °C for 10 min. Tagmentation and amplification were done following the manufacturer's instructions with TruePrep DNA library Prep Kit V2 (Vazymes, TD501). Single-end sequencing was performed by Annoroad Gene Technology, and clean reads with trimmed adapters were aligned to mm10 reference genome with the Bowtie2 (2.3.5.1) package (52). The downstream analysis pipeline was adapted from previous study (53). Briefly, broad peaks were called by the Macs2 (2.1.2) package (54) using the parameter (–nomodel –shift -100 –extsize 200 -B –broad), and differential accessed peaks were called using the Deseq2 (v.1.20.0) package (55). Differential accessed peaks were called by $|\log_2 FC| > 0.5$ and $P < 0.05$ and normalized read counts > 0. Motif enrichment analysis and peak-associated gene annotation were performed using HOMER (v4.11.1) (56) using peaks filtered by $|\log_2 FC| > 0.5$, $P < 0.05$ and normalized read counts > 0. Browser tracks were visualized by IGV Browser (v2.8.2) (57) after normalizing the read from each individual sample to its own library size. Ataqv (v1.0.0, https://github.com/ParkerLab/ataqv) package developed by the Parker Laboratory from the University of Michigan was used to perform the ATAC-seq data quality control analysis.

CUT&Tag and Analysis. The library preparation for CUT&Tag was performed as previously reported (58). In brief, 50,000 cells were extracted from isolated mouse islets by TrypLE (Thermo Fisher, 12604013). Isolated cells were washed twice with PBS. concanavalin A coated magnetic beads (Bangs Laboratories, BP531) in 500 μL Wash Buffer [20 mM Hepes, pH 7.5, 150 mM NaCl, 0.5 mM Spermidine, and protease inhibitor Cells were incubated with 10 μL of activated mixture (Roche)] for 10 min at room temperature. Cell-bound beads were collected and resuspended with 50 μL Dig-Wash Buffer (20 mM Hepes pH 7.5, 150 mM NaCl, 0.5 mM Spermidine, protease inhibitor mixture, and 0.05% digitonin) containing 2 mM EDTA, 0.1% BSA, and a 1:50 dilution of the primary antibody [anti-Pax6 (Cell Signaling Technology, 60433), anti-trimethyl-histone H3 (Lys4) (Millipore, Cat: 07-473), or normal Rabbit immunoglobulin G (IgG) (Cell Signaling Technology, 2729) and incubated at 4 °C overnight. Secondary antibody [Goat anti-Rabbit IgG (Sigma, SAB3700883) diluted at 1:100 in 100 μL of Dig-Wash Buffer was then administered into the beads and incubated for 60 min at room temperature following primary antibody removal with magnet stand (Vazyme, CM101). The preparation of pG-Tn5 adapter complex was performed according to manufacturer's instruction with Hyperactive pG-Tn5 Transposase for CUT&Tag (Vazyme, S602). Standard tagmentation and amplification were performed as reported previously (58). Amplified DNA libraries were purified with VAHTS DNA Clean Beads (Vazyme, N411) and shipped for next-generation sequencing (NGS) sequencing by Annoroad Gene Technology. Reads were filtered and mapped to mm10 genome, and peaks were then called to generate peak matrix with a pipeline similar to ATAC-seq analysis mentioned above. Differential peaks were identified by $|\log_2 FC| > 0.5$, $P < 0.05$ and normalized read counts > 0. Details of all other experimental procedures can be found in *SI Appendix, SI Materials and Methods*.

Study Approval. The animal protocol was reviewed and approved by the Animal Ethical and Welfare Committee at Institute of Radiation Medicine Chinese Academy of Medical Sciences. Human pancreas tissue was obtained between January 2016 and August 2020 from brain-dead nondiabetic and T2D donors after informed consent was obtained. The study was approved by the Tianjin First Central Hospital clinical research ethics committee.

Data Availability. All study data are included in the article and/or *SI Appendix*.

ACKNOWLEDGMENTS. This work was supported by the National Natural Science Foundation of China (grants 81830025, 81620108004, 81700699, 81700720, 91857110, and 81722012). We acknowledge the support of the National Key R&D Program of China (2019YFA0802502 and 2018-YFA0800403), the Tianjin Municipal Education Commission (2021KJ209) and the Tianjin Municipal Science and Technology Commission (17ZXMFSY00150). We also acknowledge the support of Tianjin Research Innovation Project for Postgraduate Students (2019YJSB107) and Tianjin Medical University Postgraduate Innovation Fund of "13th Five-Year Comprehensive Investment" (YJSCX201904), as well as the Zhejiang Provincial Natural Science Foundation of China (LZ21H070001). This work was also supported by the Fundamental Research Funds for the Central Universities, the Training Program of Hangzhou Key Discipline of Geriatrics, the Innovative Institute of Basic Medical Sciences of Zhejiang University, and the Construction Fund of Medical Key Disciplines of Hangzhou. We thank Dr. Zhengfan Jiang at Peking University for sharing the global STING KO mice used in this study.

1. J. C. Rathmell, Metabolism and autophagy in the immune system: Immunometabolism comes of age. *Immunol. Rev.* **249**, 5–13 (2012).
2. C. D. Bourke, J. A. Berkley, A. J. Prendergast, Immune dysfunction as a cause and consequence of malnutrition. *Trends Immunol.* **37**, 386–398 (2016).
3. R. B. Goldberg, Cytokine and cytokine-like inflammation markers, endothelial dysfunction, and imbalanced coagulation in development of diabetes and its complications. *J. Clin. Endocrinol. Metab.* **94**, 3171–3182 (2009).
4. A. Rehman, P. Pacher, G. Haskó, Role of macrophages in the endocrine system. *Trends Endocrinol. Metab.* **32**, 238–256 (2021).
5. H. Ishikawa, G. N. Barber, STING is an endoplasmic reticulum adaptor that facilitates innate immune signalling. *Nature* **455**, 674–678 (2008).
6. Q. Chen, L. Sun, Z. J. Chen, Regulation and function of the cGAS-STING pathway of cytosolic DNA sensing. *Nat. Immunol.* **17**, 1142–1149 (2016).
7. Y. Tanaka, Z. J. Chen, STING specifies IRF3 phosphorylation by TBK1 in the cytosolic DNA signaling pathway. *Sci. Signal.* **5**, ra20 (2012).
8. T. Abe *et al.*, STING recognition of cytoplasmic DNA instigates cellular defense. *Mol. Cell* **50**, 5–15 (2013).
9. H. Ishikawa, Z. Ma, G. N. Barber, STING regulates intracellular DNA-mediated, type I interferon-dependent innate immunity. *Nature* **461**, 788–792 (2009).
10. D. L. Burdette *et al.*, STING is a direct innate immune sensor of cyclic di-GMP. *Nature* **478**, 515–518 (2011).
11. T. Xia, H. Konno, J. Ahn, G. N. Barber, Deregulation of STING signaling in colorectal carcinoma constrains DNA damage responses and correlates with tumorigenesis. *Cell Rep.* **14**, 282–297 (2016).
12. A. P. West *et al.*, Mitochondrial DNA stress primes the antiviral innate immune response. *Nature* **520**, 553–557 (2015).
13. T. Li, Z. J. Chen, The cGAS-cGAMP-STING pathway connects DNA damage to inflammation, senescence, and cancer. *J. Exp. Med.* **215**, 1287–1299 (2018).
14. A. Rongvaux *et al.*, Apoptotic caspases prevent the induction of type I interferons by mitochondrial DNA. *Cell* **159**, 1563–1577 (2014).
15. M. J. White *et al.*, Apoptotic caspases suppress mtDNA-induced STING-mediated type I IFN production. *Cell* **159**, 1549–1562 (2014).
16. G. Dunphy *et al.*, Non-canonical activation of the DNA sensing adaptor STING by ATM and IFI16 Mediates NF-κB signaling after nuclear DNA damage. *Mol. Cell* **71**, 745–760.e5 (2018).
17. D. Olagnier *et al.*, Nrf2 negatively regulates STING indicating a link between antiviral sensing and metabolic reprogramming. *Nat. Commun.* **9**, 3506 (2018).
18. M. Hasan *et al.*, Chronic innate immune activation of TBK1 suppresses mTORC1 activity and dysregulates cellular metabolism. *Proc. Natl. Acad. Sci. U.S.A.* **114**, 746–751 (2017).
19. J. Bai *et al.*, Mitochondrial stress-activated cGAS-STING pathway inhibits thermogenic program and contributes to overnutrition-induced obesity in mice. *Commun. Biol.* **3**, 257 (2020).
20. J. Bai *et al.*, DsbA-L prevents obesity-induced inflammation and insulin resistance by suppressing the mtDNA release-activated cGAS-cGAMP-STING pathway. *Proc. Natl. Acad. Sci. U.S.A.* **114**, 12196–12201 (2017).
21. Y. Mao *et al.*, STING-IRF3 triggers endothelial inflammation in response to free fatty acid-induced mitochondrial damage in diet-induced obesity. *Arterioscler. Thromb. Vasc. Biol.* **37**, 920–929 (2017).
22. Y. Yu *et al.*, STING-mediated inflammation in Kupffer cells contributes to progression of nonalcoholic steatohepatitis. *J. Clin. Invest.* **129**, 546–555 (2019).
23. X. Wang *et al.*, STING expression in monocyte-derived macrophages is associated with the progression of liver inflammation and fibrosis in patients with nonalcoholic fatty liver disease. *Lab. Invest.* **100**, 542–552 (2020).
24. Y. N. Li, Y. Su, Remdesivir attenuates high fat diet (HFD)-induced NAFLD by regulating hepatocyte dyslipidemia and inflammation via the suppression of STING. *Biochem. Biophys. Res. Commun.* **526**, 381–388 (2020).
25. J. T. Qiao *et al.*, Activation of the STING-IRF3 pathway promotes hepatocyte inflammation, apoptosis and induces metabolic disorders in nonalcoholic fatty liver disease. *Metabolism* **81**, 13–24 (2018).
26. R. King *et al.*, Offspring of mice exposed to a low-protein diet in utero demonstrate changes in mTOR signaling in pancreatic islets of langerhans, associated with altered glucagon and insulin expression and a lower β-cell mass. *Nutrients* **11**, 605 (2019).
27. H. Q. Hu *et al.*, The STING-IRF3 pathway is involved in lipotoxic injury of pancreatic β cells in type 2 diabetes. *Mol. Cell. Endocrinol.* **518**, 110890 (2020).
28. A. Swisa *et al.*, PAX6 maintains β cell identity by repressing genes of alternative islet cell types. *J. Clin. Invest.* **127**, 230–243 (2017).
29. Y. Gosmain *et al.*, Pax6 is crucial for β-cell function, insulin biosynthesis, and glucose-induced insulin secretion. *Mol. Endocrinol.* **26**, 696–709 (2012).
30. M. A. Mazur *et al.*, Microphthalmia transcription factor regulates pancreatic β-cell function. *Diabetes* **62**, 2834–2842 (2013).
31. R. Fang *et al.*, NEMO-IKKβ are essential for IRF3 and NF-κB activation in the cGAS-STING pathway. *J. Immunol.* **199**, 3222–3233 (2017).
32. S. Liu *et al.*, Misfolded proinsulin impairs processing of precursor of insulin receptor and insulin signaling in β cells. *FASEB J.* **33**, 11338–11348 (2019).
33. A. Arunagiri *et al.*, Proinsulin misfolding is an early event in the progression to type 2 diabetes. *eLife* **8**, e44532 (2019).
34. M. K. Ray, S. P. Fagan, S. Moldovan, F. J. DeMayo, F. C. Brunicardi, Beta cell-specific ablation of target gene using Cre-loxP system in transgenic mice. *J. Surg. Res.* **84**, 199–203 (1999).
35. E. Conrad, R. Stein, C. S. Hunter, Revealing transcription factors during human pancreatic β cell development. *Trends Endocrinol. Metab.* **25**, 407–414 (2014).
36. Y. Hang *et al.*, The MafA transcription factor becomes essential to islet β-cells soon after birth. *Diabetes* **63**, 1994–2005 (2014).
37. N. A. Tamarina *et al.*, Small-conductance calcium-activated K+ channels are expressed in pancreatic islets and regulate glucose responses. *Diabetes* **52**, 2000–2006 (2003).
38. K. Filipsson, J. J. Holst, B. Ahrén, PACAP contributes to insulin secretion after gastric glucose gavage in mice. *Am. J. Physiol. Regul. Integr. Comp. Physiol.* **279**, R424–R432 (2000).
39. H. Cheng *et al.*, TRPM4 controls insulin secretion in pancreatic beta-cells. *Cell Calcium* **41**, 51–61 (2007).
40. Z. X. Meng *et al.*, Prostaglandin E2 regulates Foxo activity via the Akt pathway: Implications for pancreatic islet beta cell dysfunction. *Diabetologia* **49**, 2959–2968 (2006).
41. A. G. York *et al.*, Limiting cholesterol biosynthetic flux spontaneously engages type I IFN signaling. *Cell* **163**, 1716–1729 (2015).
42. J. Bai, F. Liu, The cGAS-cGAMP-STING pathway: A molecular link between immunity and metabolism. *Diabetes* **68**, 1099–1108 (2019).
43. M. Prentki, F. M. Matschinsky, S. R. Madiraju, Metabolic signaling in fuel-induced insulin secretion. *Cell Metab.* **18**, 162–185 (2013).
44. J. C. Henquin, Regulation of insulin secretion: A matter of phase control and amplitude modulation. *Diabetologia* **52**, 739–751 (2009).
45. P. Rorsman, F. M. Ashcroft, Pancreatic β-cell electrical activity and insulin secretion: Of mice and men. *Physiol. Rev.* **98**, 117–214 (2018).
46. W. Y. So, W. N. Liu, A. K. K. Teo, G. A. Rutter, W. Han, Paired box 6 programs essential exocytotic genes in the regulation of glucose-stimulated insulin secretion and glucose homeostasis. *Sci. Transl. Med.* **13**, eabb1038 (2021).
47. R. K. Mitchell *et al.*, The transcription factor *Pax6* is required for pancreatic β cell identity, glucose-regulated ATP synthesis, and Ca^{2+} dynamics in adult mice. *J. Biol. Chem.* **292**, 8892–8906 (2017).
48. S. Motoda *et al.*, Case of a novel PAX6 mutation with aniridia and insulin-dependent diabetes mellitus. *J. Diabetes Investig.* **10**, 552–553 (2019).
49. G. Yu, L. G. Wang, Y. Han, Q. Y. He, clusterProfiler: An R package for comparing biological themes among gene clusters. *OMICS* **16**, 284–287 (2012).
50. W. Luo, C. Brouwer, Pathview: An R/Bioconductor package for pathway-based data integration and visualization. *Bioinformatics* **29**, 1830–1831 (2013).
51. J. D. Buenrostro, P. G. Giresi, L. C. Zaba, H. Y. Chang, W. J. Greenleaf, Transposition of native chromatin for fast and sensitive epigenomic profiling of open chromatin, DNA-binding proteins and nucleosome position. *Nat. Methods* **10**, 1213–1218 (2013).
52. B. Langmead, S. L. Salzberg, Fast gapped-read alignment with Bowtie 2. *Nat. Methods* **9**, 357–359 (2012).
53. T. Liu *et al.*, BAF60a deficiency uncouples chromatin accessibility and cold sensitivity from white fat browning. *Nat. Commun.* **11**, 2379 (2020).
54. Y. Zhang *et al.*, Model-based analysis of ChIP-Seq (MACS). *Genome Biol.* **9**, R137 (2008).
55. M. I. Love, W. Huber, S. Anders, Moderated estimation of fold change and dispersion for RNA-seq data with DESeq2. *Genome Biol.* **15**, 550 (2014).
56. S. Heinz *et al.*, Simple combinations of lineage-determining transcription factors prime cis-regulatory elements required for macrophage and B cell identities. *Mol. Cell* **38**, 576–589 (2010).
57. J. T. Robinson *et al.*, Integrative genomics viewer. *Nat. Biotechnol.* **29**, 24–26 (2011).
58. H. S. Kaya-Okur *et al.*, CUT&Tag for efficient epigenomic profiling of small samples and single cells. *Nat. Commun.* **10**, 1930 (2019).